31 Aug 1971

Combined Thermal Weakening and Mechanical Disintegration of Hard Rock

George Bromley Clark
Missouri University of Science and Technology

T. F. Lehnhoff
Missouri University of Science and Technology

Gary F. Fenton

M. R. Patel

et. al. For a complete list of authors, see https://scholarsmine.mst.edu/min_nuceng_facwork/1231

UNIVERSITY OF MISSOURI-ROLLA

Semiannual Technical Report
Grant No. USDI H0210028 for the period
ending August 31, 1971

COMBINED THERMAL WEAKENING AND MECHANICAL DISINTEGRATION OF HARD ROCK

Rock Mechanics & Explosives Research Center
and
Department of Mechanical and Aerospace Engineering

FOREWORD

The research described in this report was initiated under Department of Defense Contract DACA-45-69-C-0087 wherein the effort was utilized for constructing the testing equipment for large blocks. The research on thermal weakening and pneumatic chipping was continued under Contract USDI H0210028 and has consisted to date of perfecting the large block testing equipment, performance of initial tests on the same, initiation of theoretical analysis of thermal elastic stresses, analysis of the application of the theory of pneumatic indentors, initiation of heat penetration studies, drop crushing tests, and correlation of data obtained from the preliminary tests performed.

Personnel working on the project are:

George B. Clark, Director, Rock Mechanics and Explosives Research Center - Principal Investigator

Terry F. Lehnhoff, Associate Professor of Mechanical Engineering - Co-investigator

Gary F. Fenton - Graduate Research Assistant (DoD)

M.R. Patel - Graduate Research Assistant

Jaw K. Wang - Graduate Research Assistant

Vernon D. Allen - Graduate Research Assistant (DoD)

CONTENTS

LIST OF FIGURES AND TABLES

Combined Thermal Weakening and Mechanical Disintegration of Hard Rock

Introduction

This investigation of the combined effects of thermal weakening and mechanical disintegration (thermomechanical fragmentation) was initiated with a view toward better understanding of the processes required for more rapidly and economically fragmenting or excavating hard rock. Boring machines for utility tunnels, transportation tunnels or mining operations may be able to utilize the advantages of processes such as thermomechanical fragmentation. Secondary fragmentation or rock crushing processes also can conceivably employ the data obtained from this study.

The research is divided into the following general areas of study:

1. Theoretical studies on the process of heat weakening including the process of heat energy coupling. Investigations to date in this area include a state-of-the-art study of the thermoelastic stresses in a homogeneous isotropic medium. The appropriate expressions have been written in the form of finite difference equations which have been programmed for computer solution. The program is currently being debugged.
2. Theoretical studies of mechanical disintegration by surface chipping and the effect of surface heating thereon. A survey has been made of existing theory for wedge and spherical indentors, which includes utilization of plastic properties of rock. Appropriate modifications will be made, equations programmed for the computer and results used to assist in the analysis of experimental results.

3. Laboratory investigations of the process parameters for thermo-mechanical fragmentation using heat assisted near surface chipping techniques. The experimental program to date has been devoted largely to equipment design and fabrication. Preliminary control drop crushing tests have been made as well as initial chipping tests on Missouri red granite.

1. Theoretical Study of Heat Weakening

The theoretical part of this research program is directed toward the calculation of the thermoelastic stress field in an infinite half-space due to a point heat source moving parallel to the surface. The actual conditions of a boring or mining operation are thus simulated. It is desirable to consider the rock properties to vary with temperature and to allow the mechanical properties to vary in two directions (orthotropic material). Many rocks possess the orthotropic characteristic at least to a first approximation. The solution of this problem has not been previously given in the literature. Carstens, et al., (Ref. 1) have concluded that the presence of thermoelastic stresses at the time the mechanical energy is imparted to the rock increases the mechanical fragmentation efficiency.

Before the thermoelastic stress field is calculated it is necessary to know the temperature distribution in the rock as a function of time. Estimates of the temperature profiles within a semi-infinite rock for a stationary heat source can be obtained from a one-dimensional transient analysis of the type by Metzger (Refs. 2, 1). He computes the convective heat transfer coefficient as

$$h = .06225 C_p G \left(\frac{\mu}{V \rho R} \right)^{.434} \left(\frac{k}{C_p \mu} \right)^{.63} \qquad (1\text{-}1)$$

and the temperature from

$$T_x = (T_f - T_R)\left\{ \operatorname{erfc}\left(\frac{X}{2\sqrt{\alpha t}} \right) - \exp\left[\left(\frac{Xh}{k_R} \right)\left(\frac{\alpha t h^2}{k_R^2} \right) \right] \right.$$
$$\left. \operatorname{erfc}\left[\left(\frac{X}{2\sqrt{\alpha t}} \right)\left(\frac{h\sqrt{\alpha t}}{k_R} \right) \right] \right\} + T_R \qquad (1\text{-}2)$$

The heat flow rate into the rock surface is obtained from

$$q = 2\pi R^2 h \left(T_f - T_s \right) \qquad (1\text{-}3)$$

where:

C_p = Specific heat of exhaust gas - Btu/lb°F

G = Mass velocity of exhaust at nozzle exit - lb/hr ft^2

h = Heat transfer coefficient in wall film - Btu/hr ft^2°F

k = Thermal conductivity of exhaust gas - Btu/hr ft°F

k_R = Thermal conductivity of rock - Btu/hr ft°F

q = Rate of heat transfer into rock surface - Btu/hr

R = Radius of rock surface target - in.

t = Time-sec

T_f = Exhaust gas temperature at wall - °F

T_R = Equilibrium rock temperature prior to heat addition - °F

T_x = Temperature in rock at distance x from surface - °F

T_s = Temperature at rock surface - °F

V = Exhaust gas velocity at nozzle exit - ft/sec

x = Linear distance into rock from surface - ft

α = Thermal diffusivity of rock - ft^2/hr

ρ = Exhaust gas density - lb/ft^3

μ = Exhaust gas viscosity - lb/hr ft

Estimates of the temperature profiles due to a moving heat source may be obtained using two-dimensional finite element codes. An iterative scheme for this purpose is being explored using a code developed by Kieth (Ref. 3).

Experimental measurements of the temperature distribution are described under the laboratory investigations section of this report.

With the temperature distribution known the thermoelastic stress field due to a moving heat source may be sought. A simplified three-dimensional finite difference solution is being programmed for the first phase of this research. A more complete study using a combination of finite element and finite difference approximations will be made during the second phase.

The heat source moving along the surface of the rock body gives rise to a jump condition (step function). A finite-difference approximation was derived for this jump condition. In order to examine the accuracy of the approximation, it was necessary to solve a simple problem involving a similar jump condition. Thus, a two-dimensional problem of heat-flow in a thin plate heated by a source moving along one of its edges was selected. The analytical solution based on the assumption of constant properties and a quasi-stationary state is given by Rosenthal (Ref. 4). The problem has been formulated in terms of finite-differences and the resulting equations are in the process of being programmed.

The temperature distribution given by Rosenthal is

for $\xi > 0$

$$T - T_o = \frac{q}{C_p a g V} \left[e^{-2\lambda V \xi} + \sum_{1}^{\infty} \frac{2}{\mu_n} e^{-\left(\mu_n + 1\right)\lambda V \xi} \cos \frac{\pi n y}{a} \right] \tag{1-4}$$

and for $\xi < 0$

$$T - T_o = \frac{q}{C_p a g V} \left[1 + \sum_{1}^{\infty} \frac{2}{\mu_n} e^{\left(\mu_n - 1\right)\lambda V \xi} \cos \frac{\pi n y}{a} \right] \tag{1-5}$$

where:

$\mu_n = \left[1 + \left(\frac{\pi n}{\lambda V a}\right)^2\right]^{\frac{1}{2}}$

ξ = Distance at the point considered from the point heat source (x direction)

q = Rate of heat flow

V = Speed of source

T = Temperature

t = Time

k = Heat conductivity

$1/(2\lambda)$ = Thermal diffusivity

C_p = Specific heat

ρ = Density

a = Plate width normal to direction of motion

g = Plate thickness

y = Distance measured from the edge of the plate normal to the direction of motion

The finite difference solution has been formulated and is being programmed according to the following scheme.

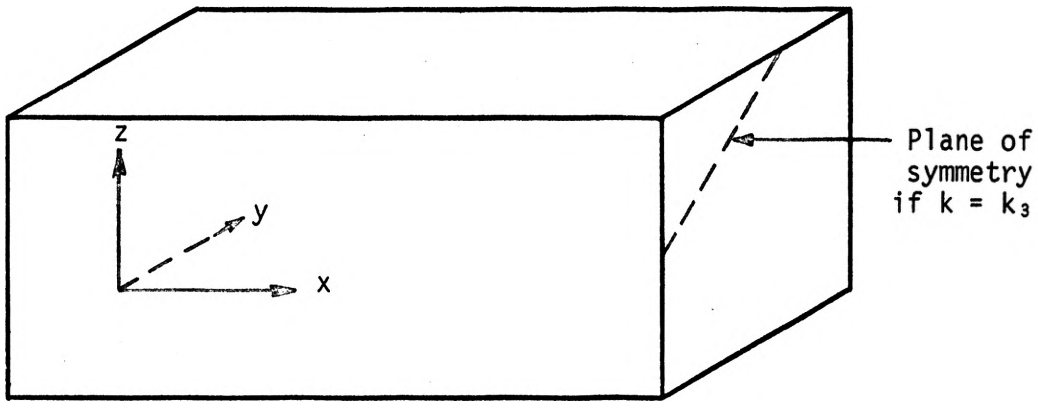

Figure 1-1. Large Rock Block

If the source is moving along the x-axis, then

$$Q = Q_0 \delta(x-Vt,\ 0,\ t) \tag{1-6}$$

Results given by Thirumalai (Ref. 5) for a one-dimensional analysis of a semi-infinite solid indicate that, since the depth of penetration is very small for the kind of rocks to be analyzed, only a small volume of the rock surrounding the heat source need be considered. Therefore, the following finite region will be considered: $0 \leq x \leq 6$, $0 \leq y \leq 0.5$, $-0.5 \leq z \leq 0.5$. In view of the symmetry, the plane xy can be treated as insulated. Thus, for the z-direction the region further reduces to $0 \leq z \leq 0.5$.

The source is assumed to be at (0.5, 0) at time t = 0 and will be allowed to traverse up to x = 5.5 with a constant velocity. The steep gradients require a rather small grid size. A constant space grid of 0.05 inches will be used. The time-step will be so selected that during one time-step, the source advances one space-step, i.e., the relation x = Vt will be used to set up the time-step

$$\Delta x = V\Delta t \text{ or } \Delta t = \frac{\Delta x}{V} \tag{1-7}$$

The total traverse of the source is xL = 5 inches. Hence, the time up to which the solution must be advanced is given by

$$t_{max} = n\Delta t = \frac{xL}{V}$$

and the total number of time-steps required is

$$n = \frac{t_{max}}{\Delta t} = \frac{\left(\frac{xL}{V}\right)}{\Delta t} = \frac{xL}{V\Delta t} \tag{1-8}$$

But since $V\Delta t = \Delta x$

$$n = \frac{xL}{\Delta x} \tag{1-9}$$

The total time-steps required corresponding to the given traverse and given space-grid size remain constant, regardless of the velocity of the source.

Three different velocities will be considered. The following table gives the related quantities for xL = 5 inches and Δx = 0.05 inches:

No.	Velocity V in./sec	t_{max} secs	Δt secs	n
1	0.5	10.0	0.1	100
2	1.0	5.0	0.05	100
3	2.0	2.5	0.025	100

For each velocity, solutions with three different Q_o values will be obtained. The total heat energy applied is given by

$$E = Q_o \, t_{max} = \frac{Q_o xL}{V} \tag{1-10}$$

or, since xL is constant,

$$E \propto \frac{Q_o}{V} \text{ , or } E_1 = \frac{Q_o}{V} \therefore Q_o = E_1 V \tag{1-11}$$

The analysis will be carried out for three different inputs of energy and for the given velocity the values of Q_o will be selected accordingly. Thus, for example, if the three energy loads are to be 50, 125, and 250 Btu/ft^2 per inch of traverse*, the combinations for V and Q_o to be used will be as follows:

Velocity V in./sec	Flux Q_o Btu/ft^{2}sec	Energy E Btu/ft^2 in traverse
0.5	25.0	50
	62.5	125
	125.0	250
1.0	50.0	50
	125.0	125
	250.0	250
2.0	100.0	50
	250.0	125
	500.0	250

* These values will be so selected that the maximum temperature of the rock does not exceed the quartz transformation temperature, i.e., approximately 570 deg C.

Mathematical formulation:

Governing equations:

$$\frac{\partial}{\partial x}\left(k\frac{\partial T}{\partial x}\right)+\frac{\partial}{\partial y}\left(k\frac{\partial T}{\partial y}\right)+\frac{\partial}{\partial z}\left(k_3\frac{\partial T}{\partial z}\right)+Q_o\,\delta(x-Vt,\,0,\,t)=\delta C(T)\frac{\partial T}{\partial t} \qquad (1\text{-}12)$$

In order to simplify the analysis, Eq. (1-12) will be replaced by the equivalent system of the homogeneous equation

$$\frac{\partial}{\partial x}\left(k\frac{\partial T}{\partial x}\right)+\frac{\partial}{\partial y}\left(k\frac{\partial T}{\partial y}\right)+\frac{\partial}{\partial z}\left(k_3\frac{\partial T}{\partial z}\right)=\delta C(T)\frac{\partial T}{\partial t} \qquad (1\text{-}13)$$

and the jump condition,

$$-k\frac{\partial}{\partial y}T(x^- - Vt,\,0,\,t)-\left\{-k\frac{\partial}{\partial y}T(x^+ - Vt,\,0,\,t)\right\}=Q_o \qquad (1\text{-}14)$$

with the continuity requirement

$$T(x^- - Vt,\,0,\,t)=T(x^+ - Vt,\,0,\,t) \qquad (1\text{-}15)$$

The (-) and (+) superscripts denote, respectively, the x-coordinates of the points just to the left and just to the right of the point x - Vt. The jump condition Eq. (14) is thus time-dependent.

Boundary conditions:

1. If the plane y = 0 is assumed to be insulated,

$$\frac{\partial}{\partial y}T(x,\,0,\,z,\,t)=0;\quad z\neq 0,\ x\neq Vt,\ t>0. \qquad (1\text{-}16a)$$

However, if the plane y = 0 is not insulated, then

$$-k\frac{\partial}{\partial y}T(x,\,0,\,z,\,t)=h\left[T(x,\,0,\,z,\,t)-T_o\right];\quad z\neq 0,\ x\neq Vt,\ t>0. \qquad (1\text{-}16b)$$

2. Due to symmetry, the plane z = 0 (or xy plane) can be treated as insulated and only the upper half (or lower half) need be considered. The corresponding boundary condition is

$$\frac{\partial}{\partial z} T\ (x,\ y,\ 0,\ t) = 0;\ y \neq 0,\ x \neq Vt,\ t > 0 \qquad (1\text{-}17)$$

3. The other (four) planes are assumed to be at ambient conditions, i.e., for these planes

$$T\ (x,\ y,\ z,\ t) = T_o;\ t > 0 \qquad (1\text{-}18)$$

Initial conditions:

$$T\ (x,\ y,\ z,\ 0) = T_o \qquad (1\text{-}19)$$

Finite Difference Formulation:

Practical considerations:

Explicit techniques will not be employed since the stability criterion requires extremely small time-steps which are prohibitive from the viewpoint of computing time. The conventional implicit techniques are unconditionally stable for all mesh ratios $\frac{\Delta t}{\Delta x^2}$. However, they require the solution of a large number of simultaneous equations at each time-step which again leads to serious computer time and storage problems. The alternating direction implicit (ADI) techniques have been shown to be highly efficient and advantageous compared to the conventional implicit techniques. For the problem to be analyzed the ADI technique developed by Douglas (Ref. 6) will be used.

For the region G: $0 \leq x \leq 6$, $0 \leq y \leq 0.5$, $0 \leq z \leq 0.5$, the number of nodes corresponding to the mesh size $\Delta x = \Delta y = \Delta z = 0.05$ are:

Along the x-direction 121

Along the y-direction 11

Along the z-direction 11

Hence, total nodes in the region G = 121 x 11 x 11.

This number, although not impossible to be handled on the computer, soon becomes prohibitive when as many as 100 time increments are involved. Therefore, it is desirable to reduce the number of total nodes to the minimum possible. If the material is assumed to be isotropic (as well as homogeneous), the diagonal plane for y = z shown dotted in the figure becomes the plane of symmetry due to the boundary conditions (1-16a) and (1-17). This assumption is justified in view of the fact that the temperature-dependent properties of the rocks to be analyzed have been obtained based on the assumption of homogeneity and isotropy.

The introduction of this additional plane of symmetry reduces the number of nodes in a plane x = constant from m^2 to $m\frac{(m+1)}{2}$; in this case, from 121 to 66. This results in a reduction of the number of nodes: for the region G, from 11 x 11 x 121 to 66 x 121, i.e., 55 x 121 nodes which is approximately a 46 percent reduction.

Governing Equations of the Reduced Problem:

Based on the preceding assumptions, the problem of the semi-infinite region is now reduced to a problem of the finite region shown below.

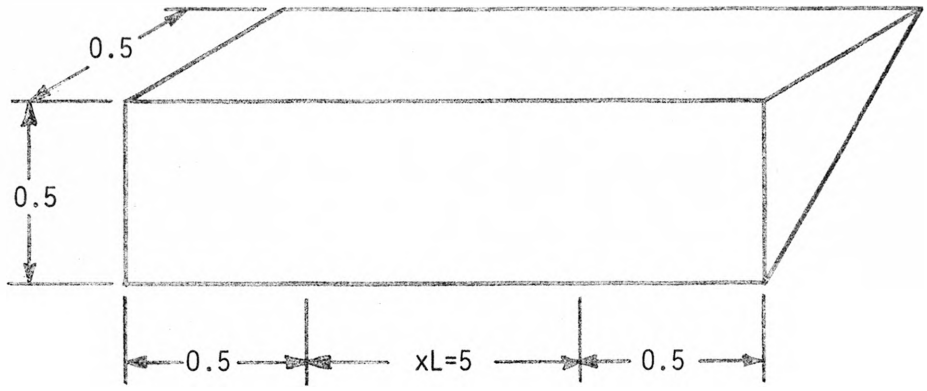

Figure 1-2. Simplified Rock Model

Governing equations: $(k = k_3)$

$$\frac{\partial}{\partial x}\left(k\frac{\partial T}{\partial x}\right) + \frac{\partial}{\partial y}\left(k\frac{\partial T}{\partial y}\right) + \frac{\partial}{\partial z}\left(k\frac{\partial T}{\partial z}\right) = \delta C(T)\frac{\partial T}{\partial t} \tag{1-20}$$

$$k\left\{\frac{\partial T}{\partial y}(x^{+} - Vt, 0, t) - \frac{\partial T}{\partial y}(x^{-} - Vt, 0, t)\right\} = Q_0 \tag{1-21}$$

$$T(x^{-} - Vt, 0, t) = T(x^{+} - Vt, 0, t) \tag{1-22}$$

Boundary conditions:

$$\frac{\partial}{\partial y} T(x, 0, z, t) = 0,\ t > 0,\ z \neq 0,\ x \neq Vt \tag{1-23}$$

$$\frac{\partial}{\partial n} T(x, C, C, t) = 0. \quad \text{For every C except C = 0 and } x = Vt \text{ simultaneously} \tag{1-24}$$

Here n is the direction of the outward normal to the plane y = z.

$$T(0, y, z, t) = T_0,\ t > 0 \tag{1-25}$$

$$T(6, y, z, t) = T_0,\ t > 0 \tag{1-26}$$

$$T(x, y, 0.5), t) = t_0,\ t > 0 \tag{1-27}$$

T_0 is the ambient temperature.

Boundary conditions (1-25, 1-26, 1-27) may be replaced by normal derivatives set equal to zero.

2. Theoretical Studies of Mechanical Fragmentation

Fragmentation processes will be studied from the viewpoint of determining the stress field created by wedge and spherical indentors. Crossed wedge bits and button bits are to be employed in the experimental part of this research. Unlike a thermoelastic problem mechanical fragmentation must be analyzed using methods of plasticity. A study of mechanical fragmentation problems in this case brings to light the fact that a rock mass will have already been subjected to the thermal weakening treatment at the time the fragmentation device is applied. This means a pattern of small cracks (due to the thermal treatment) will be present in the surface which the indentor (bit) will impact. Since the analysis of a discontinuous medium with a random distribution of cracks is a formidable problem the initial solution will be approached under the assumption that thermoelastic stresses are present but no cracking has occurred, i.e., to approximate the assumption that microfractures represent randomly distributed surfaces of plastic yielding.

Analytical studies of rock penetration by a single bit tooth have been made by Cheatham (Ref. 7) and Periseau and Fairhurst (Ref. 8) as well as Paone and Tandanand (Ref. 9) using the slip-line field method. From studies by Hill (Ref. 10) in the general case of plane strain, the governing stress equations at yield condition are hyperbolic. The characteristics of a hyperbolic differential equation can be defined as curves across which certain derivatives may be discontinuous. The directions of these characteristics can be shown in the Mohr stress diagram for Coulomb's yield criterion (Fig. 2-1).

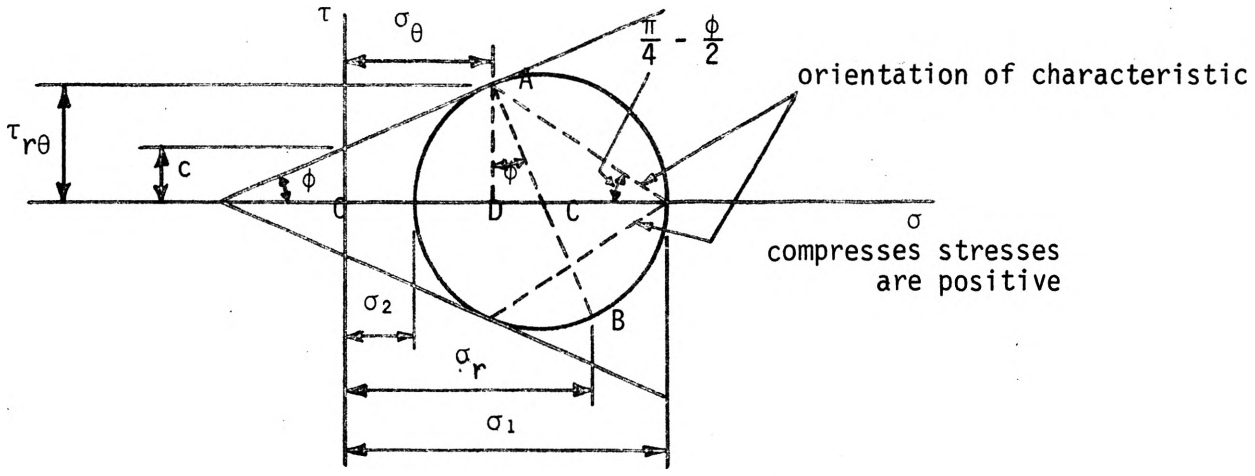

Figure 2-1. Mohr Stress Diagram for Coulomb's Yield Criterion

Courant and Friedrichs (Ref. 11) discuss solutions of hyperbolic differential equations called "simple waves" which may be applied as "simple solutions" of plane-strain, boundary-value problems in plasticity. A simple solution is one for which at least one family of characteristics is composed of straight lines. These solutions have the following properties:

1) Any straight characteristic of one family is intersected at the same angle by all characteristics of the other family.
2) All stresses are constant in an area where both families of characteristics are straight lines; this is referred to as a constant-state area.
3) The solution for an area adjacent to a constant-state area must be a simple solution.
4) Simple solutions can be joined together along the characteristics.

From the above studies, the assumed fields for the smooth bit, rough bit, and false nose situations are given in Figures 2-2 to 2-4.

A. Smooth Bit

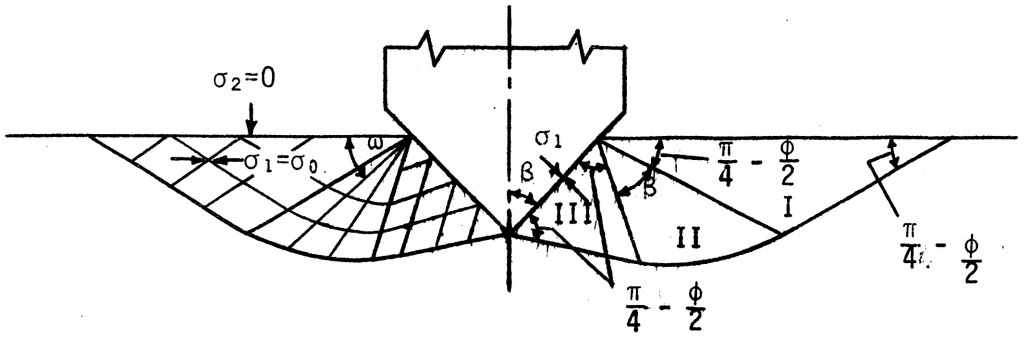

Figure 2-2. Assumed Field for Smooth Bit

B. Rough Bit

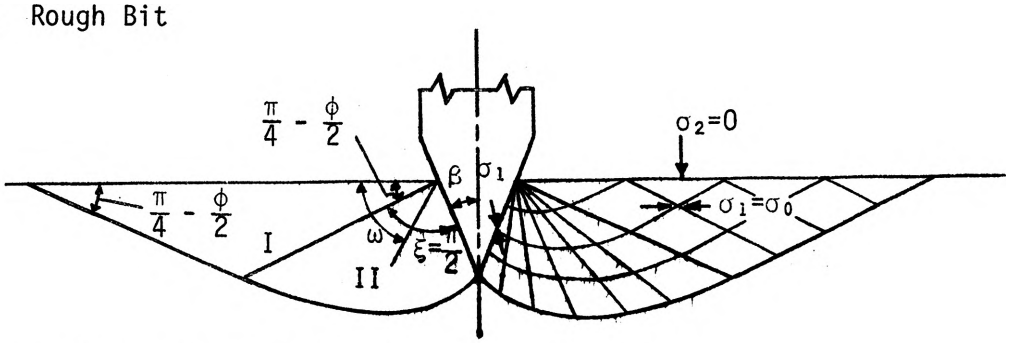

Figure 2-3. Assumed Field for Rough Bit

C. False Nose

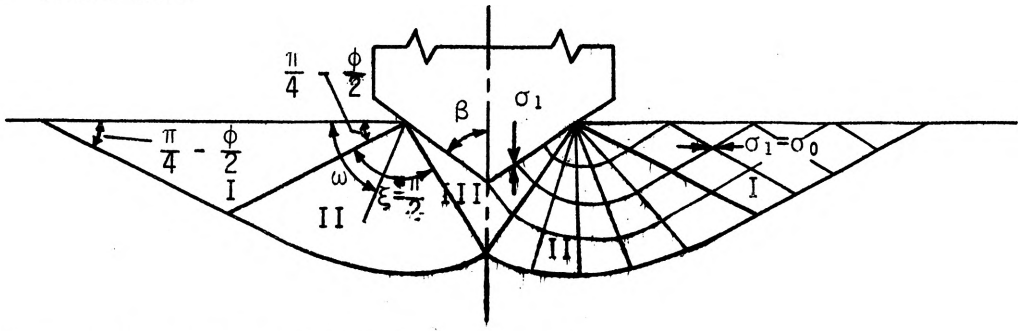

Figure 2-4. Assumed Field for False Nose

In Figures 2-2 to 2-4

β = Bit half-wedge angle ($0 \leq \beta \leq \pi/2$)

ξ = Fan angle (radial shear region)

θ = The angle specifying the direction of the major principal stress along the bit face

h = Depth of penetration

$\mu = \frac{\pi}{4} - \frac{\phi}{2}$

For smooth bit $0 \leq \beta \leq \pi/2$; $\xi = \beta$; $\theta = \pi/2 - \beta$ (2-1)

For rough bit $0 \leq \beta \leq \mu$; $\xi = \beta + \pi/2 - \mu$; $\theta = \mu - \beta$ (2-2)

For false nose $\mu \leq \beta \leq \pi/2$; $\xi = \pi/2$; $\theta = 0$ (2-3)

The stresses in regions I, II, and III are:

I. Constant state region:

$\sigma_1 = \sigma_0$ = Unconfined compressive strength (2-4)

$\sigma_2 = 0$ (2-5)

II. Radial shear region (not a function of r):

$$\tau_{r\theta} = (1 + \sin \phi)\, c e^{2(\omega-\alpha) \tan \phi} \tag{2-6}$$

$$\sigma_1 = \frac{c}{\tan \phi} \left[\frac{1 + \sin \phi}{1 - \sin \phi} e^{2(\omega-\alpha) \tan \phi} - 1 \right] \tag{2-7}$$

$$\sigma_2 = \frac{c}{\tan \phi} \left[e^{2(\omega-\alpha) \tan \phi} - 1 \right] \tag{2-8}$$

III. Constant state region:

$$\sigma_1 = \frac{\sigma_0}{2 \sin \phi} (1 + \sin \phi)\, e^{-2\beta \tan \phi} - 2 c \cot \phi \tag{2-9}$$

σ_2 (can be obtained from Mohr diagram) (2-10)

The general equation for the force-penetration characteristic is

$$\frac{F}{h\sigma_0} = \frac{\tan \beta}{\tan \phi \tan \mu} \left\{ \left[\frac{1 + \cot 2\theta \, (1 + \cot \beta \tan 2\theta) \sin \phi}{(1 + \sin \phi)} \right] \right. \exp(2 \xi \tan \phi) - \tan^2 \mu \left. \right\} \qquad (2\text{-}11)$$

The solution of the problem for the dull-tooth shapes may be obtained by combining the solutions obtained for the simple basic shapes (Ref. 7).

3. Laboratory Investigations

The primary objective of the experimental phase of the research is to determine the specific energy of breakage of hard rock with and without thermal weakening. The tests are being run on thirty-inch cubic blocks of rock. Six rock types have been selected as representative of those which are difficult and costly to excavate by conventional techniques. The rocks have also been selected to span the range from very good response to thermal weakening to very poor response. The subject rocks are Missouri red granite, Minnesota charcoal granite, Buena black granite, Kitledge pink granite, Sioux quartzite and Dresser basalt. The thermal energy for the first phase of the research is being provided by a flame jet torch. For the second phase a radiant heater (infrared) will be employed. The mechanical energy is provided by a pneumatic hammer.

The test apparatus shown in Figure 3-1 is designed to pass the thirty-inch cubic blocks in front of the pneumatic hammer and flame jet heat source. The actual conditions that will occur when a heat source and mechanical fragmentation device are passed over a tunnel face during a boring or mining operation are reasonably well simulated by the test machine.

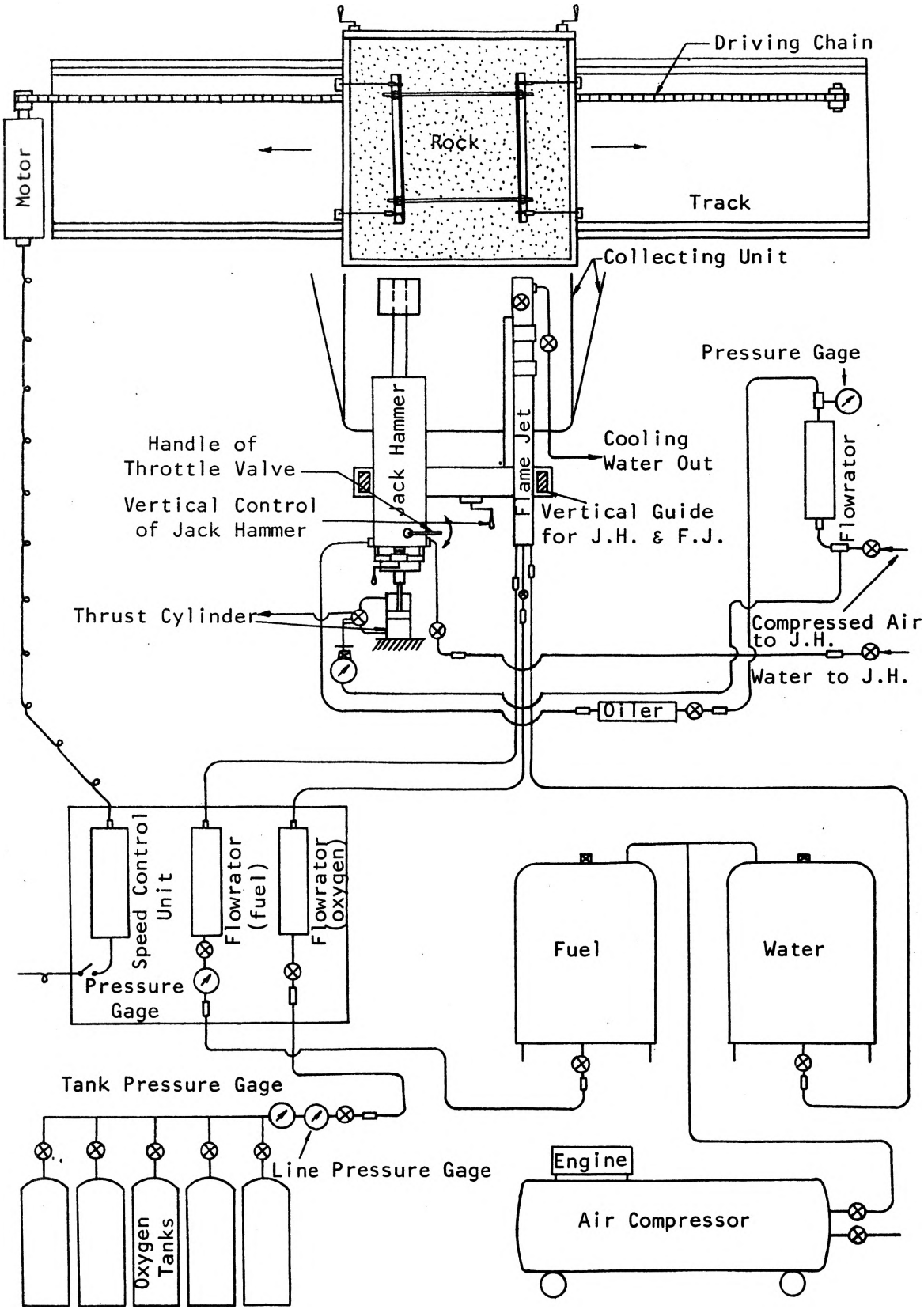

Figure 3-1. Schematic of Experimental Apparatus for Thermomechanical Fragmentation

The speed of traverse of the heat source and the mechanical fragmentation device can be selected in the range from 0.0 to 2.0 inches per second. The pressure cylinder permits the thrust of the pneumatic hammer to be varied from 0.0 to 300 pounds. However, thrusts greater than 80-90 pounds cause the bit to drill a hole in the conventional sense rather than remove a layer from the surface for each traverse as is planned in this work. Initial tests for the purpose of measuring the pneumatic hammer energy output indicate (Table 3-1) that a maximum thrust consistent with the necessary transverse movement is desirable. Estimates of the pneumatic hammer energy output were obtained using the relation due to Pfleider and Lacabanne (Ref. 12).

$$E = \frac{P^{3/2} A^{3/2} S}{W^{\frac{1}{2}}} \qquad (3\text{-}1)$$

where:

E = Energy output - in.-lb

P = Mean effective air pressure on working face of piston - lb/in.^{2}

A = Area of working face of piston - in.^{2}

S = Length of power stroke of piston - in.

W = Weight of piston - lb

The above conclusion is generally in agreement with the work of Lundquist and Anderson (Ref. 13), although their study was for conventional drilling. Subsequent pneumatic hammer energy measurements will be made to substantiate the optimum operating conditions. The block diagram of Figure 3-2 and Table 3-1 show how the pneumatic hammer energy output was determined. The manufacturer's value for working stroke was used in the table because the values obtained in the initial tests were somewhat inconsistent. The experimental values of stroke were obtained from measuring the number of drill steel revolutions and the known piston rotation per inch of linear travel.

Table 3-1 Pneumatic Hammer Energy Output

Throttle Setting	Stroke (in)	Thrust (lb)	Mean Effective Pressure (from 1st run) (psi)	Mean Effective Pressure (from 2nd run) (psi)	Energy (1st run data) ($\frac{ft\text{-}lb}{min}$)	Energy (2nd run data) ($\frac{ft\text{-}lb}{min}$)
#1	$2\frac{9}{16}$	13.0		11.9		52.3
		27.8	10.6	11.6	43.8	50.2
		55.0		11.2		48.0
		83.4				
#2	$2\frac{9}{16}$	13.0	19.8	19.8	112.6	112.6
		27.8	19.8	20.5	112.6	118.2
		55.0	19.2	21.8	107.0	129.8
		83.4	19.5		109.8	
#3	$2\frac{9}{16}$	13.0	26.4	19.8	173.3	112.6
		27.8	27.7	24.4	186.4	154.2
		55.0	28.4	25.1	193.1	160.4
		83.4	29.7		206.8	
#4	$2\frac{9}{16}$	13.0	26.4	28.4	173.3	193.1
		27.8	27.1	28.4	179.8	193.1
		55.0	26.4	26.4	173.3	173.3
		83.4	26.4		173.3	

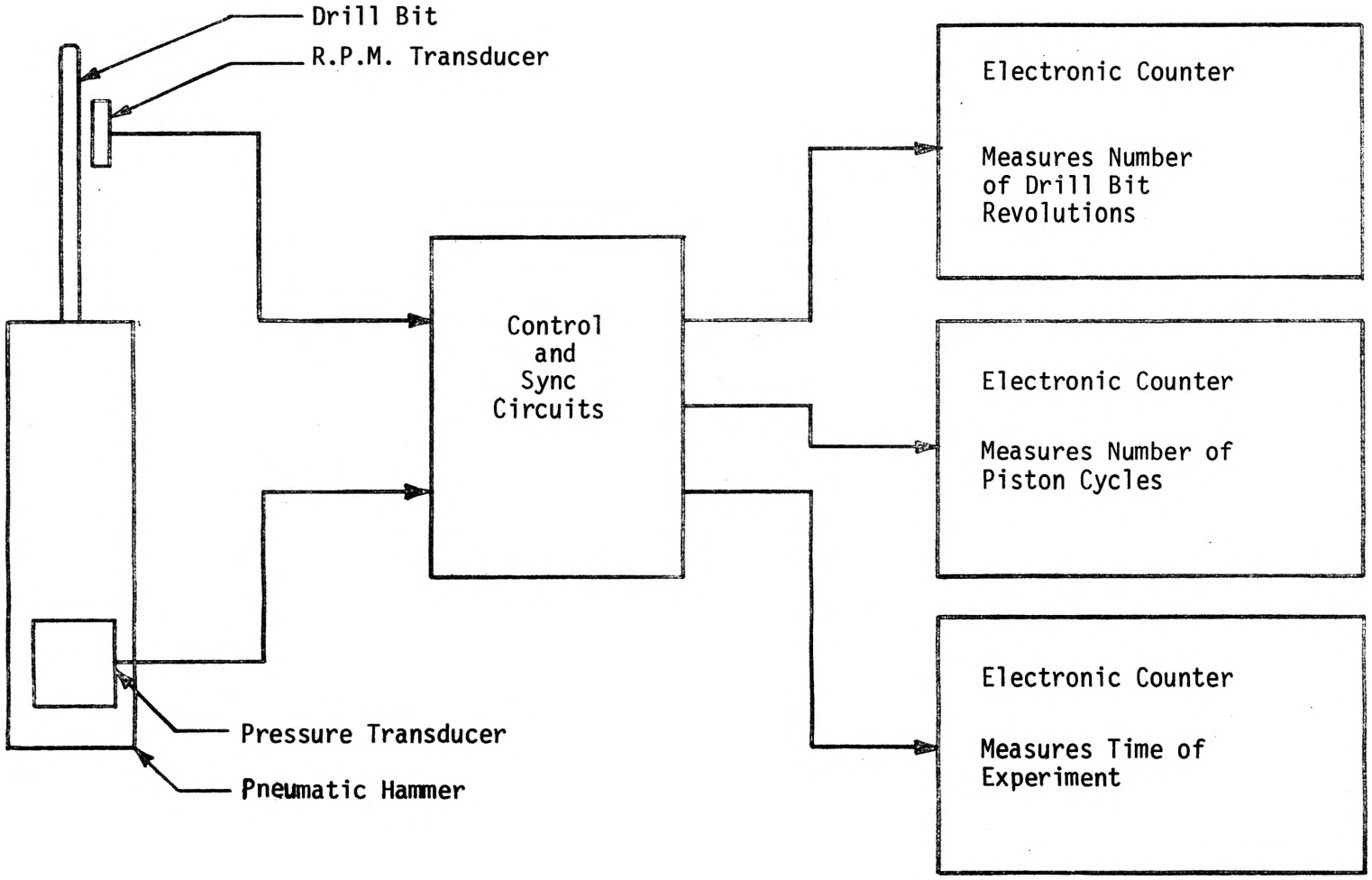

Figure 3-2. Pneumatic Hammer Energy Output Instrumentation

The effects of heat energy coupling can be determined by comparison with standards established from the results of tests without thermal weakening. The specific energy of breakage is determined by comparing the particle size distribution of the collected rock chips with particle size distributions obtained from drop weight (crushing) tests. Samples of the test materials (1/2 inch by 2 by 1/4 inch diameter cylinders) can be crushed using a known amount of energy input from a drop weight test machine (see Figure 3-3).

The results from several known energy inputs (drop heights) are plotted on semi-log cumulative particle size distribution paper as shown in Figure 3-4. The particle size distributions from the chipping tests with and without heat weakening can be plotted on this same sheet as shown. The specific energy of chipping can be obtained by comparison with the curves from the drop weight tests. Gross and Zimmerly (Refs. 14, 15) have shown that particle size is a fairly accurate measure of the surface area formed during the fragmentation process. Further, they have shown that the energy required for fragmentation (the formation of surface area) is directly related to particle size in accordance with the Rittinger law of crushing. Felts, Clark and Yancik (Ref. 16) have employed the Rittinger, Kick and Bond theories to determine the specific energy of breakage for explosives. The Rittinger theory can be expressed mathematically as:

$$E = K_r \left[\sum_{i=1}^{n} pct_i \frac{1}{d_i} - \frac{100}{d_o} \right] \qquad (3\text{-}2)$$

where:

E = Energy used in breakage

d_o = Average diameters of screen fractions of rock particles

pct_i = Percent weight of diameter d_i

n = Number of screens

$\sum pct_i$ = 100 percent

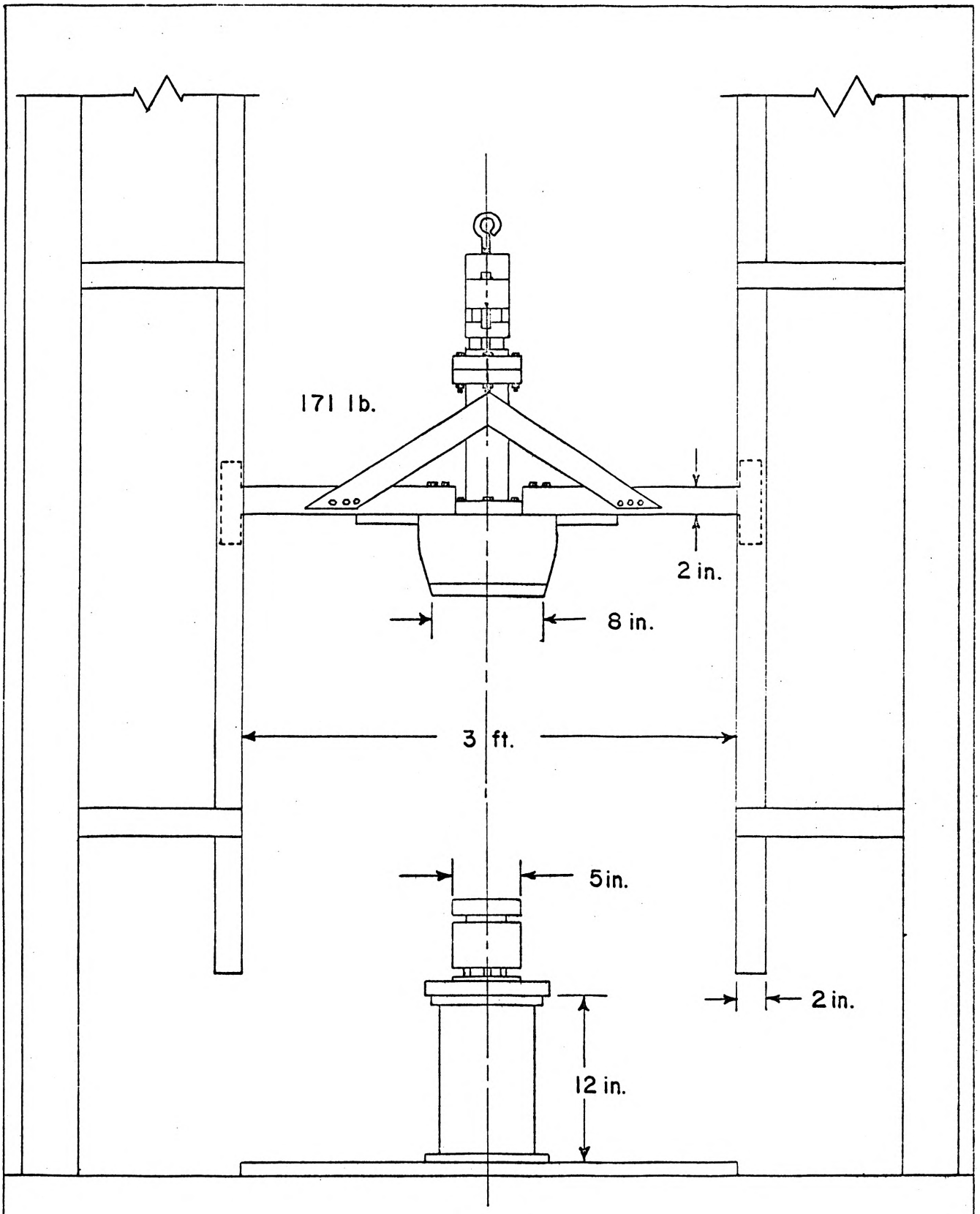

Figure 3-3

DROP WEIGHT TESTER

SCALE 0.1" = 1.0"

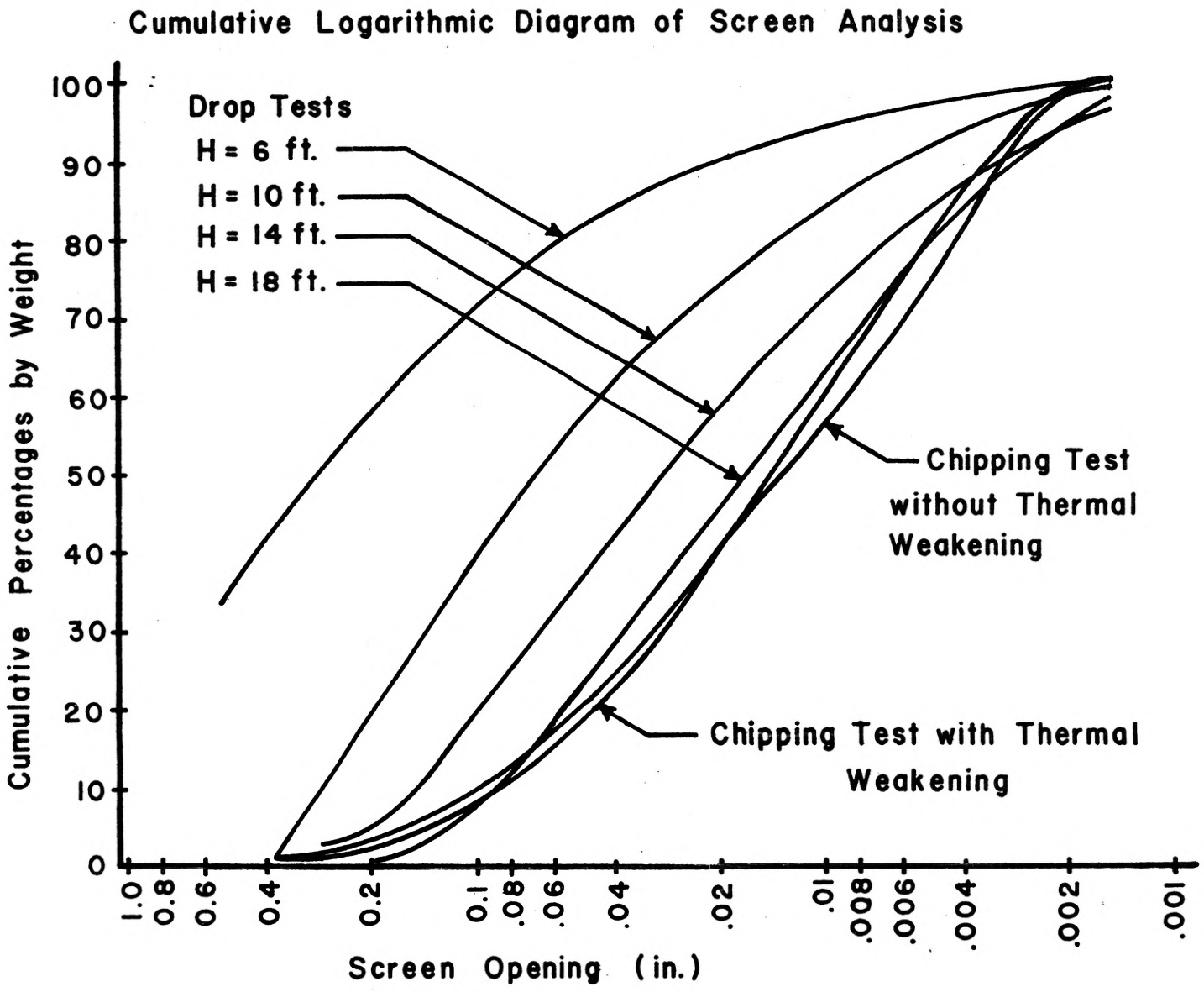

Figure 3-4. Particle Size Distribution

The equation is used to determine the constant k_r from the drop crushing tests. A computer program has been written for these calculations. This value in turn is used to determine the specific energy of breakage of the particles from the chipping tests. The efficiency of the fragmentation process can then be calculated by dividing this specific energy by the maximum available energy from the fragmentation device with and without heat assistance. The energy output of the flame jet torch is estimated as approximately 450,000 Btu/hr for optimum operating conditions. The same conditions of operation are used for each test. The energy input to the rock is varied by adjusting the distance the flame is located from the rock surface and by varying the speed of traverse.

Preliminary surface temperature measurements at a specified point on the rock surface for three traverse speeds, three offset conditions and the maximum torch distance from the rock are shown in Figures 3-5, 3-6, and 3-7. The block diagram of Figure 3-8 illustrates the method by which these temperatures were obtained. The sensing element was of the resistance type and was installed with ceramic cement. Additional temperature measurements will be made to cover the complete range of torch distances and traverse speeds. These measurements were made using Missouri red granite. Other rock types will be tested to determine if measurable differences can be observed (as a function of mineral content). The surface temperatures will be correlated with measurements made at various depths in order to better define the heat penetration characteristics. Similar tests were run by Browning, et al., (Ref. 17) using embedded thermocouples. Measurements made using the flame jet heat source will be compared with similar measurements for the radiant heat source during the second phase of work.

The theoretical studies discussed earlier will utilize the temperature distributions to calculate thermal stresses in the rock.

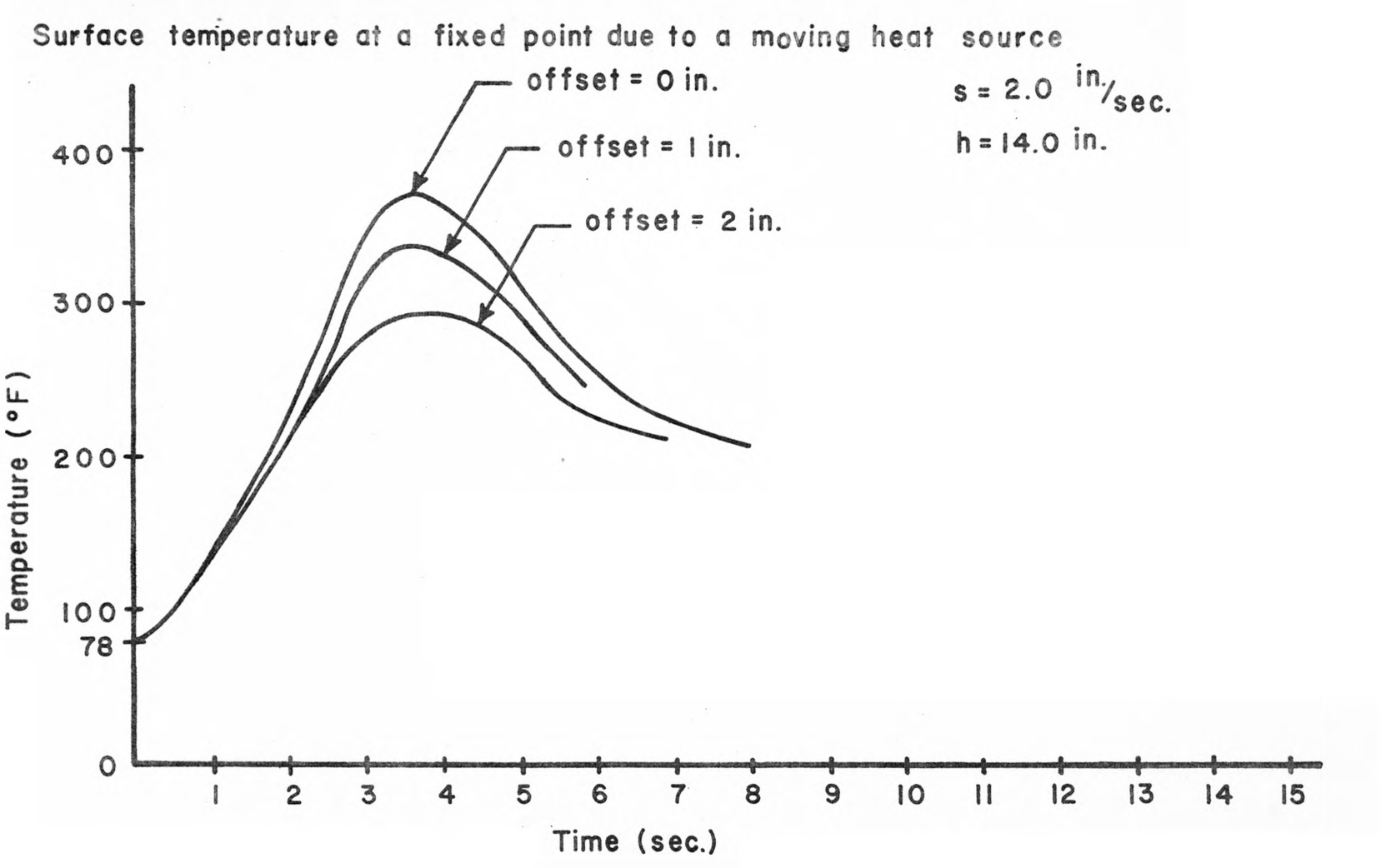
Surface temperature at a fixed point due to a moving heat source
offset = 0 in.
offset = 1 in.
offset = 2 in.
s = 2.0 in./sec.
h = 14.0 in.
Temperature (°F)
400
300
200
100
78
0
1
2
3
4
5
6
7
8
9
10
11
12
13
14
15
Time (sec.)

Figure 3-5

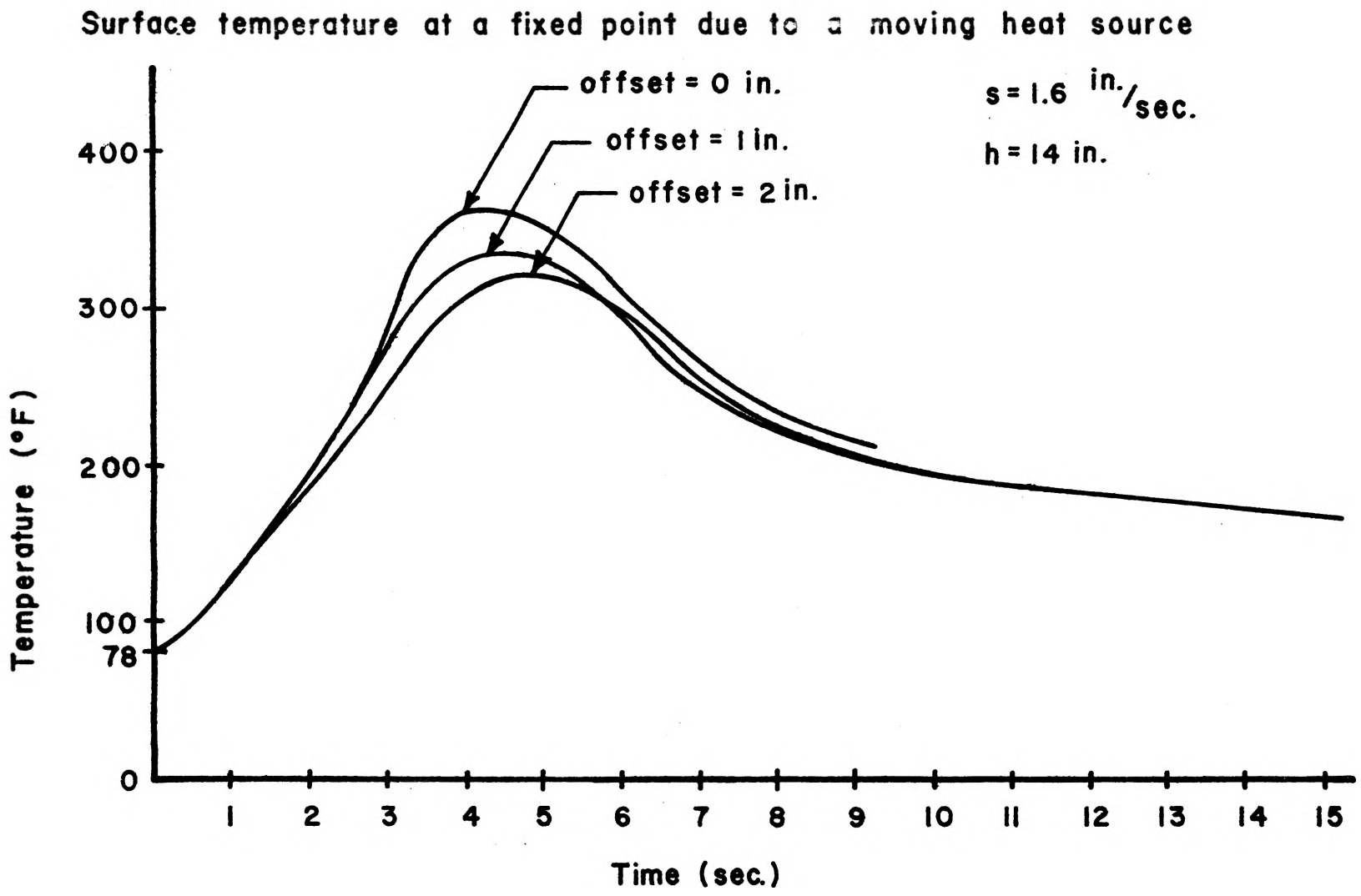
Surface temperature at a fixed point due to a moving heat source
offset = 0 in.
offset = 1 in.
offset = 2 in.
s = 1.6 in./sec.
h = 14 in.
Temperature (°F)
400
300
200
100
78
0
1
2
3
4
5
6
7
8
9
10
11
12
13
14
15
Time (sec.)

Figure 3-6

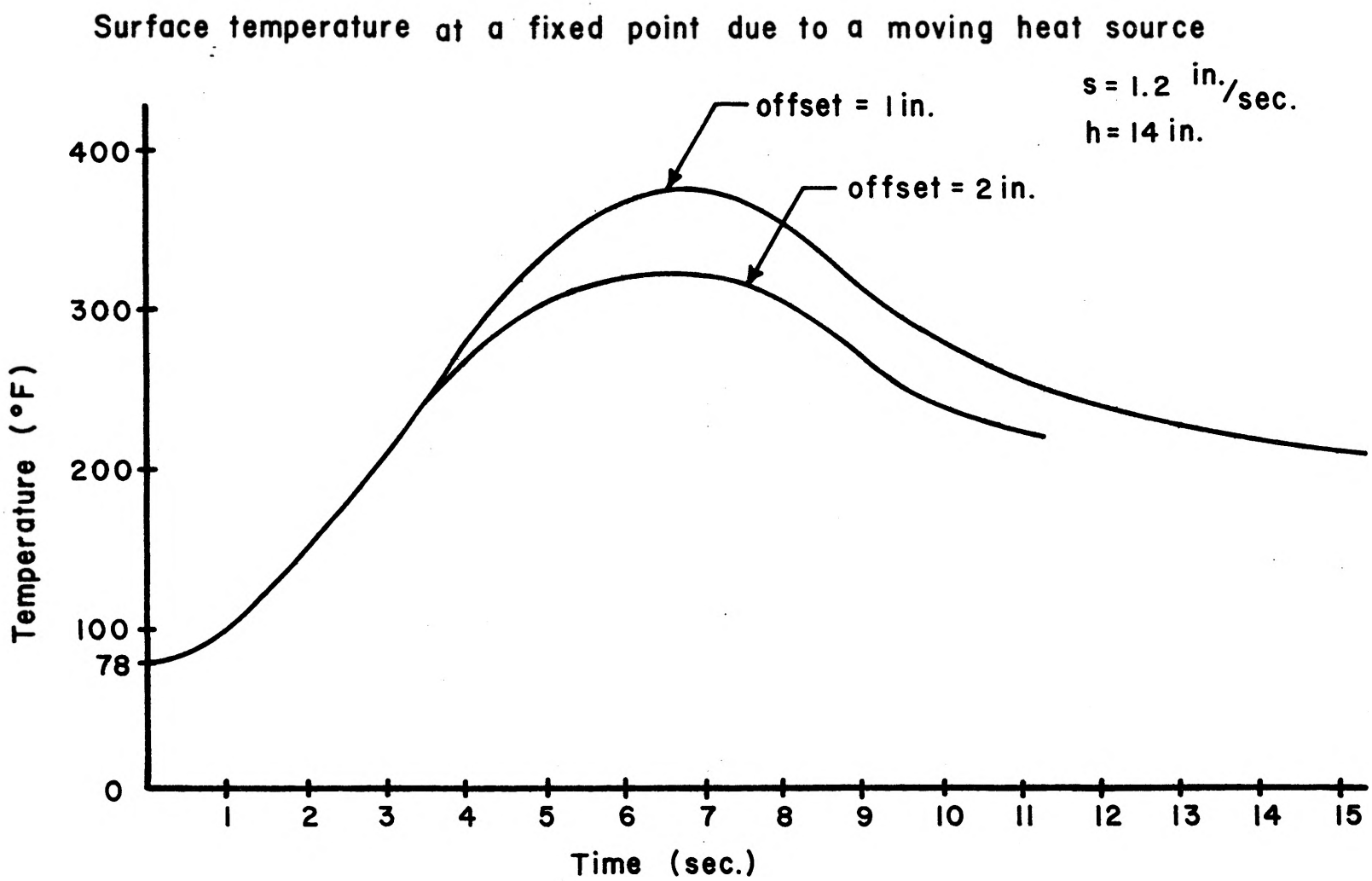
Surface temperature at a fixed point due to a moving heat source
s = 1.2 in./sec.
h = 14 in.
offset = 1 in.
offset = 2 in.
Temperature (°F)
400
300
200
100
78
0
1
2
3
4
5
6
7
8
9
10
11
12
13
14
15
Time (sec.)

Figure 3-7

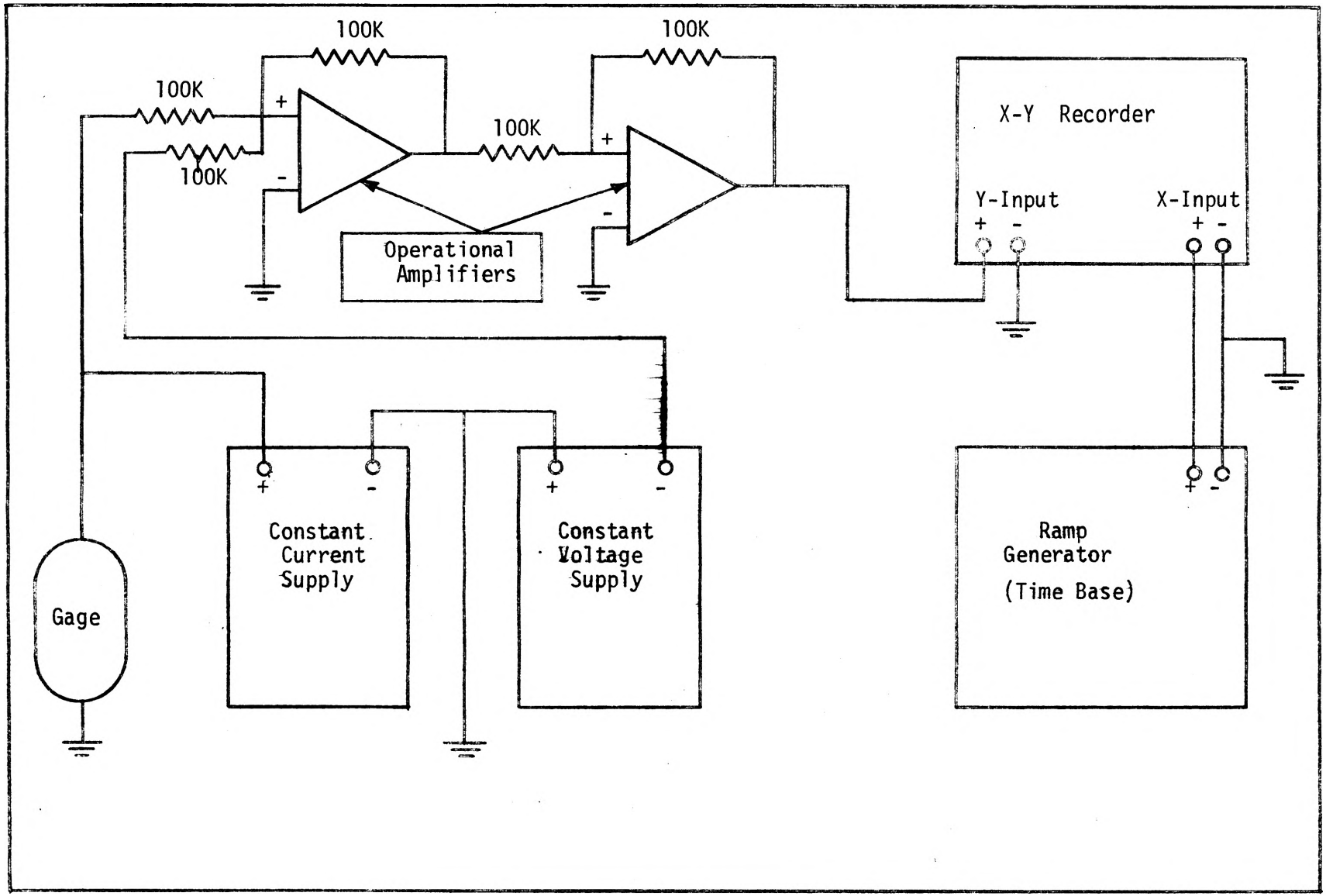

Figure 3-8. Temperature Measurement Instrumentation

References

1. Carstens, J.P.; Davidson, W.R.; Brown, C.A.; Smith, A.R.; and McGarry, F.J., "Heat Assisted Tunnel Boring Machines," UARL Report J-970802-12 or FRA-RT-71-63, Sept. 1970.

2. Metzger, D.E., "Spot Cooling and Heating of Surfaces with High Velocity Impinging Air Jets," TR No. 52 for ONR Contract NONR 225(13), Stanford University, April 1962.

3. Keith, H.D., "Two-Dimensional Finite Element Temperature Code," unpublished research, University of Missouri-Rolla.

4. Rosenthal, D., "The Theory of Moving Sources of Heat and Its Application to Metal Treatments," ASME Trans., Nov. 1946, pp. 852-866.

5. Thirumalai, K., "Process of Thermal Spalling Behavior in Rocks - An Exploratory Study," Proceedings Eleventh Symposium on Rock Mechanics, June 1969, pp. 705-727.

6. Douglas, J., "Alternating Direction Methods for Three Space Variables," Numerische Mathematils, Vol. 4, 1962, pp. 41-63.

7. Cheatham, J.B., "An Analytical Study of Rock Penetration by a Single Bit Tooth," Eighth Annual Drilling and Blasting Symposium, Oct. 2, 1958.

8. Pariseau, W.G. and Fairhurst, C., "The Force-Penetration Characteristic for Wedge Penetration into Rock," International Jour. Rock Mech. and Mining Sci., Vol. 4, No. 2, pp. 165-180.

9. Paone, J. and Tandanand, S., "Inelastic Deformation of Rock Under a Hemispherical Drill Bit," Seventh Symposium on Rock Mechanics, June 1965, pp. 149-174.

10. Hill, R., The Mathematical Theory of Plasticity, Clarendon Press, Oxford, 1950.

11. Courant, R., and Friedrichs, K.O., Supersonic Flow and Shock Waves, Wiley Interscience, New York, 1948.

12. Pfleider, E.P. and Lacabanne, W.D., "Higher Air Pressures for Down the Hole Percussive Drills," Mine and Quarry Engr., Vol. 27, Nov. 1961, pp. 496-501.

13. Lundquist, R.G. and Anderson, C.F., "Energetics of Percussive Drills - Longitudinal Strain Energy," USBM RI No. 7329, Dec. 1969.

14. Gross, J. and Zimmerly, S.R., "Crushing and Grinding, II - Relation of Measured Surface of Crushed Quartz to Sieve Sizes," AIME Trans., Vol. 87, 1930, pp. 27-34.

15. Gross, J. and Zimmerly, S.R., "Crushing and Grinding, III - Relation of Work Input to Surface Produced in Crushing Quartz," AIME Trans., Vol. 87, 1930, pp. 35-50.

16. Felts, L.L.; Clark, G.B.; and Yancik, J.J., "A Laboratory Method of Determining the Thermodynamic Efficiency of High Explosives," AIME Trans., Vol. 8, No. 3, March 1956, pp. 318-322.

17. Browning, J.A.; Horton, W.B.; and Hartman, H.L., "Recent Advances in Flame Jet Working of Minerals," Seventh Rock Mechanics Symposium, pp. 281-311.

Semiannual Technical Report

Grant No. USDI H0210028 for the period
ending August 31, 1971

ERRATA

Page	Location	is	should be
4	Eqs. (1-4), (1-5)	C_p	$C\rho$
5	Line 10	C_p	C
8	Eq. (1-12)	$\delta(x-vt, o, t)$ $\delta C(T)$	$\delta(x-vt, o, o; t)$ $\rho C(T)$
	Eq. (1-13)	$\delta C(T)$	$\rho C(T)$
	Eq. (1-14)	(x^-vt, o, t)	$(x^-vt, o, o; t)$
		(x^+vt, o, t)	$(x^+vt, o, o; t)$
	Eq. (1-15)	(x^-vt, o, t)	$(x^-vt, o, o; t)$
		(x^+vt, o, t)	$(x^+vt, o, o; t)$
	Line 13	Eq. (14)	Eq. (1-14)
11	Eq. (1-20)	$\delta C(T)$	$\rho C(T)$
	Eqs. (1-21), (1-22)	(x^+vt, o, t)	$(x^+vt, o, o; t)$
		(x^-vt, o, t)	$(x^-vt, o, o; t)$
	Eq. (1-27)	t_0	T_0
15	Fig. 2-2	$\frac{\pi}{4}-\frac{\phi}{2}$ at the bit	$\frac{\pi}{4}+\frac{\phi}{2}$
15	Fig. 2-3	$\xi = \frac{\pi}{2}$	ξ
17	Eq. (2-11)	cot $z\Theta$	cos $z\Theta$
30	Ref. 6	Mathematils	Mathematik